Sensitivity analysis of a marine gasoline engine: from power to emissions

Luigia MOCERINO[a,1], Vincenzo PISCOPO[a], and Antonio SCAMARDELLA[a]
[a] *University of Naples "Parthenope", Department of Science and Technology, Centro Direzionale Isola C4 80143, Naples, Italy*

Abstract. Numerical simulations currently represent a valid aid to assess the performance of marine engines. Anyway, most of past applications generally focused on large supercharged 4-stroke diesel engines, while few results are available in the literature for fast outboard engines, generally installed onboard recreational crafts. Therefore, a case study on a fast outboard diesel engine (4T, 6300 rpm, 350 hp) is currently provided and discussed. The simulations are performed in the Ricardo Wave environment, where NO_X and CO emissions are estimated, in addition to the typical engine performances. The data, required for the model calibration, were obtained from the engine manufacturer datasheets, as well as from a set of available sea trials. Nevertheless, not all parameters were available, so as some of them were selected based on past experience or in accordance with similarly sized diesel engines, after performing a preliminary sensitivity analysis. As concerns the assessment of NO_X and CO emissions, different simulation methods are embodied to assess the chemical equilibrium in the combustion chamber and investigate the relevant incidence in terms of time effort amount, and estimated results. Current simulations reveal to be also useful to model dual fuel (gasoline/natural gas) engines and evaluate the impact of this type of alternative plant on consumption and air emissions.

Keywords. Outboard engine, simulation, emissions, dual fuel

1. Introduction

The maritime sector greatly contributes to the emission of air pollutants such as Sulphur Oxide (SO_X), Nitrogen Oxide (NO_X), Carbon monoxide (CO), water pollutants (noise, thermal, discharges), and greenhouse gases (GHG) [1]-[4]. In this respect, in the last decade, several solutions have been considered to reduce harmful emissions and obtain possible improvements in engine and ship performances [5]-[8]. The approach to this problem can be of two types: experimental and simulative.

Simulation has been used in engineering for decades as a support for design and engineering. Marine propulsion system simulations can be used for many purposes such as ship performance and maneuvering analysis and control systems [9]-[13]. Engine simulation models can be ordered into three classes, 0D (or single-zone), quasi-dimensional (or multi-zone), and multidimensional models [14]. Although the first model has the capability of predicting engine performance accurately, it is lacking in the prediction of exhaust emissions. Multi-dimensional models, instead, provide a considerable amount of information but the results may vary according to the formulation

[1] Corresponding Author, E-mail: luigia.mocerino@unina.it

of initial or boundary conditions [14]. The quasi-dimensional models combine some of the benefits of simple 0D models and multi-dimensional models. These models solve mass and energy equations and require drastically less computing resources compared to multi-dimensional models. The two-zone model is the most useful multi-zone model; in this model, the cylinder contents are split into a non-burning zone of air and another homogeneous zone where fuel is burned. This combustion model, unlike the 0D ones, allows the evaluation of gaseous emissions with the semi-empirical equations and is used for predicting the performance and emission characteristics of a conventional engine [14]. The gasoline or spark-ignition (SI) internal combustion engine is based on the Otto cycle and an externally supplied ignition. It burns an air/fuel mixture and in the process, it transforms the fuel chemical energy into kinetic energy [15]. The engine compression ratio can be different, according to design configuration but it generally lies between 7 and 13 bar. Because the knock resistance of the fuel is limited, extreme compression pressures and high temperatures in the combustion chamber must be avoided to prevent the spontaneous and uncontrolled detonation of the air/fuel mixture [15], [17].

Based on previous remarks, the paper explores the employment of engine simulation to investigate the performance and emissions of pleasure craft equipped with outboard engines. After framing an introduction on the engine simulation, the engine case test and the engine model are presented. After the first phase of construction and validation of the simulation model, the engine model is analyzed in terms of NO_X and CO emissions. Finally, as some parameters required for the construction of the model were unavailable, a sensitivity analysis is carried out to investigate the relevant impact in terms of emissions of air pollutants.

2. Case study: data sheet and sea trials

The engine used as a case study is the 4 stroke Suzuki DF350A [18]. The technical datasheet of the engine is shown below (Table 1). The boat has a length of 9,6 m and is equipped with two Suzuki DF350 outboards. The maximum speed is 54 kn combined with a displacement equal to 2500 kg, without the engines [19]. According to the sea trials available in the literature [19], Figure 1 provides the consumption and speed curves as a function of the engine revolutions per minute.

Table 1. Engine datasheet [18]

Datasheet	**4T Double overhead camshaft/6 cyl (V 55°)/4 valves**
Displacement	4390 cc
Power	257,4 kW
Compression ratio	1:12
Optimal use regime	5700 – 6300 rpm
Bore x stroke	98 x 97 mm
Fuel/ Recommended fuel	Unleaded fuel/ RON94/AK189
Starting	Electric start
Weight	339 kg
Exhaust	Through propeller shaft
Propeller	12”-31.5”

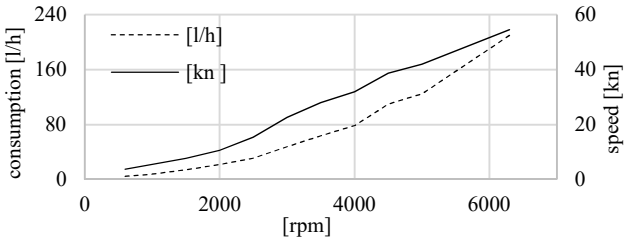

Figure 1. Engine simulation model.

3. Construction of the model

The engine has been modeled in the simulation environment considering its main parts, namely the cylinders, injectors, inlet/outlet ducts, and valves. Each block has been characterized by the relevant main dimensions, initial conditions, and characteristics of the fluid present within. Both the *in* and *out* of the engine are connected with the environment, initially under standard pressure and temperature conditions, so the air pressure and temperature are equal to 1 bar and 300 K, respectively. As regards the fuel type used during the simulation, the technical datasheet of the engine declares the RON94 (Table 1) [18] as recommended fuel. Since the RON94 (Research Octane Number) has not been available in our library of pre-characterized fuels, the RON95 has been used.

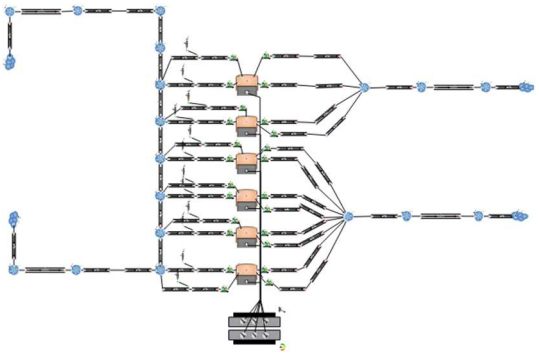

Figure 1. Engine simulation model.

The model reflects the structure of the real engine and therefore has six cylinders, each one with four valves, as well as the whole structure including pipes and injectors. The main geometric characteristics of the cylinders are reported in Table 2.

Table 2. Main geometric characteristics of the cylinders

Geometry	Value
Stroke/Bore [mm]	97/98
Head area Multiplier	1,10
Compression ratio	12
Clearance Height [mm]	1,45
Connecting rod length [mm]	143

In addition to these constructive and geometric quantities, the following parameters should be set: (i) initial average surface temperature of the top of the piston (T_{piston} set to 520 K); (ii) initial average surface temperature of the cylinder liner (T_{liner} set to 430 K); (iii) average initial surface temperature of the head (T_{head} set to 520 K); (iv) average initial surface temperature of the intake valves (T_{intake} and $T_{exhaust}$ set to 520 K). The valves, schematized as in Figure 2, have been characterized based on the type, the reference diameter, and the lift and flow profile. In this application, in the absence of true data, typical profiles were used. Figure 3 (left side) shows the lift profile as a function of the crank angle, while Figure 3 (right side) shows the flow coefficient profile as a function of the lift/diameter ratio.

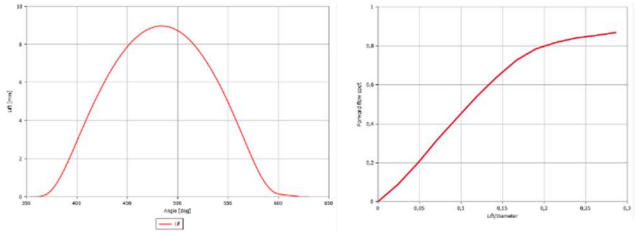

Figure 3. Lift (left) and flow coefficient profile (right).

In absence of more detailed information, a proportional type of injectors has been used. This element continuously injects fuel into the connected flow element, according to a fuel/air ratio provided by the user. The software automatically adjusts the refueling rate, keeping it proportional to the instantaneous air mass at the injection point so that the air-fuel ratio is continuously controlled based on user-specified input. Other data to be fixed are the temperature of the mixture, the diameter of the holes, the angle of the spray, and the fraction of liquid that evaporates. For all these parameters literature data have been used. A Spark Ignition (SI) Wiebe combustion sub-model was applied to each cylinder of the engine. The SI Wiebe function is widely used to describe the rate of the mass of fuel burned in thermodynamic calculations. It is a primary combustion model commonly used in SI engines. The inputs to the combustion model are: (i) the position of the combustion point where there is 50% of the burnt mass fraction (After the Top Dead Center-ATDC); (ii) the duration of combustion (from 10% to 90% of the burned mass fraction); (iii) the exponent in the Wiebe function that controls the shape of the Wiebe curve. In our model, the Wiebe parameters have been set at 5°, 15°, and 2°, respectively. A modified form of the Chen-Flynn correlation is used to model friction in the simulation model. The correlation has four terms for accessory friction (a constant term); load dependence, a term that varies with peak cylinder pressure; hydrodynamic friction, a third term linearly dependent on mean piston velocity; windage losses, and a fourth term quadratic with mean piston velocity. The overall formula is reported by eq. (1):

$$FMEP = A_{cf} + \frac{1}{ncyl}\sum_{i=1}^{ncyl} B_{cf}\left(p_{max}\right)_i + C_{cf}\left(S_{fact}\right)_i + Q_{cf}\left(S_{fact}\right)_i^2 \quad (1)$$

where: all the coefficients are reported in Table 3, p_{max} is the maximum cylinder pressure, n_{cyl} is the number of cylinders and S_{fact} is obtained according to eq. (2):

$$S_{fact} = RPM \cdot stroke/2 \quad (2)$$

where *stroke* is the cylinder stroke and RPM is the engine speed revolution for a minute.

Table 3. The coefficient for the modified form of the Chen-Flynn correlation

Coefficient friction	Value	Units
A_{cf}	0,35	bar
B_{cf}	0,004	-
C_{cf}	400	Pa.min/m
Q_{cf}	1	$Pa.min^2/m^2$

The NOx model assigns an initial NOx concentration and considers the NO "prompt" obtained from the correlation of the data reported by Fenimore (1970) [20] which provides the ratio between the NO prompt and the NO equilibrium as a function of the equivalence ratio. All NOx is assumed to be in the form of NO during the rapid formation phase, as well as the thermal phase described below by the extended *Zeldovich NOx* formation mechanisms [21]. The entire burned zone is treated as an open and layered system in which further NOx formation takes place depending on the temperature, pressure, and equivalence ratio of the portion being burned. The concentration of NO overtime is resolved using an open system in which the above elementary reactions are used at a constant rate [21]. For the first reaction equation, the rate constants, R_1 and $R_{2/3}$, are given by eq. (3) and (4):

$$R_1 = A \cdot ARC1 \cdot e^{(T_a \cdot \frac{AERC1}{T})} \tag{3}$$

$$R_{2/3} = A \cdot e^{(T_a/T)} \tag{4}$$

where A is the pre-exponent constant; $ARC1$ and $AERC1$ are the Arrhenius pre-exponent and exponent multiplier, set equal to 1,10 and 1,21, respectively; T_a is the activation temperature for the reaction, T is the temperature of the burned zone. The calculation stops when the temperature in the burned area reaches a level low enough to make the kinetics inactive and the total NO emission doesn't change. The CO emissions sub-model predicts CO production during combustion and exhaust in an engine cylinder element.

4. Results

Once every single element has been inserted and characterized and the engine simulator is assembled, the simulations can be carried out. In absence of inconsistencies between the boundary conditions, the duct diameters, and the combustion parameters, the simulation provides a large amount of information on the operating conditions of the engine, as can be highlighted in Figure 4.

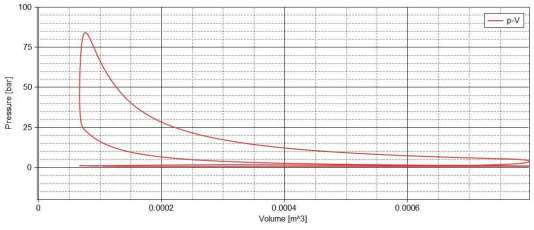

Figure 4. p-V diagram.

The possible validation was carried out on power and consumption. In particular, the power obtained in the simulation environment at 6300 rpm is equal to 238 kW, with a 7% error as regards the rated power of the engine. Additional validation of the simulation model was carried out concerning the consumption obtained during sea trials between 4000 and 6300 rpm (63-100% of the load approximately), see Figure 5.

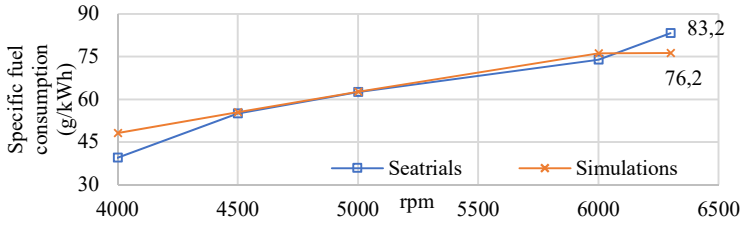

Figure 5. Specific fuel consumption validation.

The NO_X flow rate at 6300 rpm is equal to 1,39 kg/h, based on the simulation results. This value can easily be compared with the emission factor provided by EMEP-EEA (2019) of 25,8 kg/fuel [22]. Taking into account the specific consumption obtained with the simulation of approximately 76 l/h equivalents to approximately 0,057 t/h and dividing the pollutant flow rate obtained by this value, an emission factor of approximately 24,4 (approximately -5,5%) is obtained. As regards the CO emission, the results have shown how the uncertainties related to the combustion parameters such as the duration of combustion or the position in which 50% of the mass of fuel burns significantly affected the obtained results. In this respect, by varying this parameter between 5^O and 15^O, the results range from a minimum of 4,5 to a maximum of 8,0 kg/h. Even the use of a fuel with a RON other than the prescribed one affects the results: by switching from a RON100 to a RON91 the CO flow rate drops from 3,0 to 2,3 kg/h. In any case, the model returns an emission factor never higher than 150 kg/t_{fuel}, therefore always well below the 348 kg/t_{fuel} expected for 4-stroke petrol by EMEP-EEA [22].

5. Sensitivity analysis

Given the large number of parameters involved that were not available from the datasheet during the construction of the model, a sensitivity analysis of the data was necessary [23]-[25]. From a careful observation of the input parameters, the following quantities were chosen for the aforementioned analysis: duration of combustion (a), the position of the burnt 50% mass fraction (ATDC) (b); the fraction of liquid that evaporates during injection (c); variation of the inlet temperature and pressure (d). The output results of the sensitivity analysis are: (i) the main properties of combustion and pressure in the cylinder (only for the first two analyzes), (ii) torque and/or power, (iii) emissions, ppm of NO_X, and CO. The results show that by tightening the combustion duration, a slightly higher power, reduced consumption, and a lower CO emission (in contrast to the NOx emissions) in accordance with Heywood (2018) is obtained [21]. The position of the 50% fraction of burned mass, to which the whole combustion process is sensitive, was initially set at 8^O ATDC and has been altered by $\pm 3^O$. The 5^O position ATDC determines a higher power peak as the quantity of fuel present in the combustion chamber is greater, with optimization of consumption and CO emissions. The liquid fraction that evaporates immediately after injection, has been set equal to 0,3 and it was varied between 0.1 and 0,5. Based on current results, this parameter has a low incidence on torque and consumption. The inlet temperature has been altered of ±5 K related to the default value of 298 K. The results show a slight increase in torque when the temperature drops and a slight decrease in the same with a higher input temperature. Consumption, on the other hand, remains substantially unchanged (Table 4). Finally, the inlet pressure has been altered of ±5% related to the 1 bar of default. The power obtained with a 5% increase in

inlet pressure reaches 251 kW, which reduces the error of the simulation model to 3%. Also, the fuel flow rate, in this case, is closer to the real case of 83,2 l/h, see Table 4.

Table 4. Results of the sensitivity analysis

		Power	Torque	SFC	CO	NO_X	Fuel flow
		[kW]	[Nm]	[g/kWh]	[ppm]	[ppm]	[l/h]
Burning duration	10°	237,6	360,2	240,9	3713,3	886,1	76,2
	15°	236,3	358,2	241,5	3759,5	813,4	76,0
	20°	234,8	355,9	243,1	3798,1	765,8	76,0
	25°	232,6	352,6	245,3	3837,6	739,5	76,0
	30°	230,0	348,6	248,0	3954,0	731,3	76,0
Location of 50% burnt point	5°	238,8	361,9	239,7	3534,0	985,7	76,2
	8°	236,3	358,1	241,7	3759,9	813,1	76,0
	11°	232,4	352,2	245,5	4058,8	679,6	76,0
T setting variation	293 K	237,5	360,1	241,3	3728,5	801,8	76,3
	298 K	236,0	358,6	241,5	3758,6	812,1	76,1
	303 K	236,2	357,9	241,7	3766,8	814,5	76,0
p setting variation	-5%	220,2	333,8	245,5	3757,5	763,5	72,0
	0%	234,9	356,1	242,2	3800,3	829,3	75,7
	5%	252,0	381,9	238,3	3782,4	873,6	80,0

6. Future work and conclusions

From the sensitivity analysis provided in Section 5, it can be verified that by increasing the air pressure entering the cylinders, the performance of the engine in simulation approaches the real one. This evidence, since the engine is not supercharged, suggests further insights into the diameters of the ducts and the characteristics of the inlet valves to the cylinders. In fact, by increasing the inlet airflow the results obtained could be realigned to the result obtained with an inlet pressure of 1,05.

Therefore, by correcting the geometry of the ducts and valves and possibly cross-referencing the results of the other sensitivity analyses, the simulation model can be further refined. The next step will be the simulation of the same engine, powered by natural gas following what the technology and real application suggest with the aim of estimating the reduction of air pollutant emissions [15],[26],[27].

References

[1] Dodero, M., Bertagna, S., Marino, A., & Bucci, V. (2020). Performance in-live of marine engines: A tool for its evaluation. Applied Sciences, 10(16), 5707.

[2] Mocerino, L., Quaranta, F., & Rizzuto, E. (2018). Climate changes and maritime transportation: A state of the art. Technology and Science for the Ships of the Future, 1005-1013.

[3] Mocerino, L., & Rizzuto, E. (2019, August). Preliminary approach to the application of the Environmental Ship Index. In Sustainable Development and Innovations in Marine Technologies: Proceedings of the 18th International Congress of the Maritime Association of the Mediterranean (IMAM 2019), September 9-11, 2019, Varna, Bulgaria (p. 285). CRC Press.

[4] Coppola, T., Lorenzo, F. D., & Mocerino, L. (2019). The irradiated noise underwater by the ships: A state of the art. Nautical and Maritime Culture, from the Past to the Future, 90-97.
[5] Altosole, M., Campora, U., Mocerino, L., & Zaccone, R. (2022) An innovative variable layout steam plant for waste heat recovery from marine dual-fuel engines. Ships and Offshore Structures, in press.
[6] Altosole, M., Balsamo, F., Campora, U., & Mocerino, L. (2021) Marine dual-fuel engines power smart management by hybrid turbocharging systems. Journal of Marine Science and Engineering, 9(6), 663.
[7] Pennino, S., Gaglione, S., Innac, A., Piscopo, V., & Scamardella, A. (2020). Development of a new ship adaptive weather routing model based on seakeeping analysis and optimization. Journal of Marine Science and Engineering, 8(4), 270.
[8] De Luca, F., & Pensa, C., (2012). Unconventional interceptors in still water and in regular waves: Experimental study on resistance reduction and dynamic instability, in: *NAV International Conference on Ship and Shipping Research*. p. 216369.
[9] Altosole, M., Benvenuto, G., Figari, M. (2005). Performance prediction of a planing craft by dynamic numerical simulation. Proceedings of the 7th Symposium on High Speed Marine Vehicles, 2005 Conference, HSMV 2005, 105-111.
[10] Altosole, M., Benvenuto, G., Figari, M., (...), Michetti, S., & Ratto, M. Real time simulation of the propulsion plant dynamic behaviour of the Aircraft Carrier "Cavour". Conference Proceedings of the Institute of Marine Engineering, Science and Technology - INEC 2008: Embracing the Future.
[11] Altosole, M., Boote, D., Brizzolara, S., & Viviani, M. (2013). Integration of numerical modeling and simulation techniques for the analysis of towing operations of cargo ships. International Review of Mechanical Engineering, 7(7), 1236-1245.
[12] Ircani, A., Martelli, M., Viviani, M., (...), Podenzana-Bonvino, C., & Grassi, D. (2016). A simulation approach for planing boats propulsion and manoeuvrability. International Journal of Small Craft Technology, 158, B-27-B-42.
[13] Acanfora, M., Altosole, M., Balsamo, F., Micoli, L., & Campora, U. (2022). Simulation Modeling of a Ship Propulsion System in Waves for Control Purposes. Journal of Marine Science and Engineering, 10(1), 36.
[14] Chidambaram K, Thulasi V (2016) Two zone modeling of combustion, performance and emission characteristics of a cylinder head porous medium engine with experimental validation. Multidiscip Model Mater Struct 12(3):495–513.
[15] Reif, K. (2015). Gasoline engine management. Bosch Professional Automotive Information, DOI, 10, 978-3.
[16] Stapf, K. G., Seebach, D., Pischinger, S., Adomeit, P., & Ewald, J. (2009). Modeling and Simulation of Gasoline Auto-Ignition Engines. IFAC Proceedings Volumes, 42(26), 40-47.
[17] Mocerino, L., Soares, C. G., Rizzuto, E., Balsamo, F., & Quaranta, F. (2021). Validation of an Emission Model for a Marine Diesel Engine with Data from Sea Operations. Journal of Marine Science and Application, 20(3), 534-545.
[18] https://marine.suzuki.it/modelli.aspx
[19] https://www.boatmag.it/37077-suzuki-df40-ari-arkos-21-test-motore-gommone/
[20] Fenimore, C. P. “Formation of Nitric Oxide in Premixed Hydrocarbon Flames”. Proceedings of the Combustion Institute Vol. 13 (1970): 373
[21] Heywood, J. B. (2018). Internal combustion engine fundamentals. McGraw-Hill Education.
[22] EMEP EEEA 2019. EMEP/EEA air pollutant emission inventory guidebook. Copenhagen, Denmark: European Environment Agency.
[23] Benvenuto, G., Campora, U., Altosole, M., & Balsamo, F. (2021). Numerical modelling and analysis of the ambient conditions influence on the performance of a marine diesel engine. In Developments in Maritime Technology and Engineering (pp. 463-474). CRC Press.
[24] Rakopoulos, C. D., & Glakoumis, E. G. (2006). Sensitivity analysis of transient diesel engine simulation. Proceedings of the Institution of Mechanical Engineers, Part D: Journal of Automobile Engineering, 220(1), 89-101.
[25] Pal, P., Probst, D., Pei, Y., Zhang, Y., Traver, M., Cleary, D., & Som, S. (2017). Numerical investigation of a gasoline-like fuel in a heavy-duty compression ignition engine using global sensitivity analysis. SAE International Journal of Fuels and Lubricants, 10(1), 56-68.
[26] Altosole, M., Benvenuto, G., Campora, U., Laviola, M., & Zaccone, R. (2017). Simulation and performance com-parison between diesel and natural gas engines for ma-rine applications. Proceedings of the Institution of Mechanical Engineers, Part M: Journal of Engineering for the Maritime Environment, 231(2), 690-704
[27] Altosole, M., Buglioni, G., Figari, M., (2014). Alternative Propulsion Technologies for Fishing Vessels: a Case Study. International Review of Mechanical Engineering, 8 (2), 296–301. https://doi.org/10.15866/IREME.V8I2.459.